Di- and Trimanganese *N*,*N*′-Dicyclohexylformamidinate Complexes

Aparna Kasani,[a] Ruppa P. Kamalesh Babu,[a] Khalil Feghali,[a] Sandro Gambarotta,*[a] Glenn P. A. Yap,[c] Laurence K. Thompson,*[b] and Regine Herbst-Irmer[d]

Abstract: The reaction of $[MnCl_2(thf)_2]$ with the *N*,*N*′-dicyclohexylformamidinate anion gave two remarkably different results depending on the nature of the amidinate alkali metal countercation. The reaction with the lithium salt affords a mixed-valence Mn–oxo cluster $[Mn_3(CyNCHNCy)_6OLi]\cdot 2THF$ (**1**), formed by the deoxygenation of THF. In the case of the potassium salt, a dinuclear complex $[\{(CyNCHNCy)Mn\}_2(\mu\text{-}CyNCHNCy)_2]$ (**2**) was formed; it has a highly distorted structure. The complexes **1** and **2** are both extremely sensitive to oxygen. Reaction of **2** with dry O_2 afforded the dinuclear complex $[\{Mn(CyNCHNCy)_2\}_2(\mu\text{-}O)]_2\cdot 2THF$ (**4**).

Keywords: clusters · manganese · molecular orbitals · semiempirical calculations

Introduction

Amidinate anions are versatile ligands and have been widely used in transition metal and lanthanide chemistry to form complexes which display a wide variety of reactivity (Ziegler–Natta catalysis,[1] dinitrogen fixation,[2] M–M bonds of unusual shortness,[3] etc.). In addition, as a result of their ability to adopt two different bonding modes to metals (bridging[4] or chelating[5]), these ligands are suitable substrates with which to study the factors that promote or disfavor the formation of very short M–M contacts. For example, the employment of a homogeneous series of cyclohexylamidinate derivatives has shown that steric contacts between the amidinate substituents determine the type of bonding mode[3c] and possibly the magnitude of the intermetallic separation in dinuclear species. As a result of the broad interest, amidinate complexes are known for the large majority of transition[1–6] and non-transition metals,[7] lanthanides,[8] and actinides.[9] To our knowledge, divalent manganese provides one of the few cases for which only one example of an amidinate complex has been reported so far.[10] This is surprising because divalent manganese complexes often display a high-spin d^5 electronic configuration and, in a similar manner to d^4 Cr^{II} complexes, they should be, at least in principle, suitable substrates with which to study the occurrence of unusually short M–M contacts.[3c] On the other hand, the tetrahedral coordination environment, one of the most commonly encountered with Mn^{II} complexes, could make the occurrence of short Mn–Mn contacts problematic with bridging bulky amidinates. Thus, in order to probe how the well-established binucleating ability of the *N*,*N*′-dicyclohexylformamidinate anion and its well-known tendency to stabilize extremely short M–M contacts[2b, 3c] will cope with the poor tendency of Mn^{II} to form short Mn–Mn contacts, we have now attempted the preparation and characterization of *N*,*N*′-dicyclohexylformamidinate manganese derivatives.

Last but not least, amidinate anions might be versatile supporting ligands with which to model the complexity of the reactivity with dioxygen. The identification of manganese sites in photosystem II (PSII), in superoxide dismutase, as well as in other enzymes has stimulated considerable research into the coordination of medium-valent manganese[11] and the reactivity of these complexes with O_2. The manganese cluster in PSII of plants is known to contain metal ions connected mainly to nitrogen donor atoms[12] and in various combinations of oxidation states (II, III, and IV). The superoxide dismutase is basically a Mn^{III} porphyrin derivative.[13] Thus, ligand systems based on nitrogen-donor atoms, such as amide or amidinate, can be reasonably expected to increase the reactivity of these metals and to provide suitable substrates for the investigation into their reactivity with O_2. This type of reactivity might perhaps have some relevance to the biochemistry of manganese.[14]

[a] Prof. S. Gambarotta, A. Kasani, R. P. Kamalesh Babu, K. Feghali
Department of Chemistry, University of Ottawa
Ottawa, Ontario K1N 6N5 (Canada)
Fax: (+1) 613-562-5170
E-mail: sgambro@ oreo.chem.uottawa.ca

[b] Prof. L. K. Thompson
Department of Chemistry, Memorial University
St. John's, Newfoundland, A1B 3X7 (Canada)

[c] Prof. G. P. A. Yap
X-ray Laboratory, Faculty of Science, University of Ottawa
Ottawa, Ontario K1N 6N5 (Canada)

[d] Dr. R. Herbst-Irmer
Institut für Anorganische Chemie der Universität
Tammannstrasse 4, D-37075 Göttingen (Germany)

  0947-6539/99/0502-0577 $ 17.50+.50/0

Experimental Section

All operations were performed under an inert atmosphere with standard Schlenck techniques. Solvents were dried with the appropriate drying agents and distilled prior to use. Crystalline [Li(CyNCHNCy)] · hexane[15a] was prepared by treating the samples of pure *N*,*N*′-dicyclohexylformamidine[15b] with *n*-butyllithium in hexane. $[MnCl_2(thf)_2]$[16] was prepared according to published procedures. Infrared spectra were recorded on a Mattson 9000 FTIR instrument from Nujol mulls prepared in a drybox. Elemental analyses were carried out with a Perkin Elmer 2400 CHN analyzer. Samples for magnetic susceptibility measurements were prepared inside a drybox and sealed into calibrated tubes. Magnetic measurements were carried out with a Gouy balance (Johnson Matthey) at room temperature. The magnetic measurements at variable temperature were performed with a low-field SQUID magnetometer. The magnetic susceptibility of a sample of **2** (10.8 mg) was measured in a field of 68.5 Gauss (or 6.85 mT), while a sample of **4** (18.0 mg) was measured in a field of 50 Gauss (or 7.1 mT) from 4.2 to 273 K. The magnetic moments were calculated by standard methods[17] and corrections for underlying diamagnetism were applied to the data.[18]

$[Mn_3(CyNCHNCy)_6OLi]\cdot 2THF$ (**1**): A pale pink suspension of $[MnCl_2(thf)_2]$ (2.6 g, 9.7 mmol) in THF (125 mL) was treated with lithium *N*,*N*′-dicyclohexylformamidinate (5.8 g, 19.3 mmol). Soon after the addition, the solid disappeared to give a clear pale yellow solution. After a few minutes, a pale colored solid precipitated. The reaction mixture was boiled until it became a clear yellow solution (30 min) and subsequently it was concentrated to a small volume (50 mL). The solution was allowed to stand at room temperature for 3 days to give pale yellowish orange crystals. Yield: 2.8 g (1.8 mmol, 55 %); IR (Nujol mull, NaCl): $\tilde{\nu}$ = 1659 (m), 1575 (s), 1447 (s), 1335 (s), 1310 (s), 1292 (s), 1258 (s), 1235 (m), 1181 (m), 1148 (s), 1104 (s), 1060 (s), 1027 (m), 986 (s), 960 (m), 916 (m), 887 (s), 841 (m), 783 (m), 721 (m), 657 (s) cm^{-1}; elemental analysis calcd for $C_{86}H_{148}LiMn_3N_{12}O_4$ (%): C 65.13, H 9.41, N 10.60; found C 64.93, H 10.02, N 10.27; μ_{eff} = 5.86 μ_B per formula unit.

$[\{(CyNCHNCy)Mn\}_2(\mu\text{-}CyNCHNCy)_2]$ (**2**): Neat *N*,*N*′-dicyclohexylformamidine (4.6 g, 22.2 mmol) was dissolved in THF (125 mL) and stirred with excess KH (35 % dispersion in paraffin, 1.5 g, 37.5 mmol). The suspension was boiled for 10 min and filtered to remove excess KH. The filtrate was transferred with a cannula to a flask containing a suspension of $[MnCl_2(thf)_2]$ (93.0 g, 11.1 mmol) in THF (75 mL). The reaction mixture was boiled for 10 min and then evaporated to dryness in vacuo. The residue was extracted with THF (100 mL) and filtered to remove potassium chloride. Pale yellow crystals were obtained after concentration to a small volume (50 mL) and standing at room temperature for 48 h. Yield 2.5 g (2.7 mmol, 48 %); IR (Nujol mull, NaCl): $\tilde{\nu}$ = 1662 (m), 1555 (s), 1449 (s), 1366 (s), 1344 (s), 1319 (s), 1285 (s), 1264 (s), 1223 (s), 1176 (s), 1154 (s), 1118 (s), 1086 (s), 1076 (s), 1027 (m), 986 (s), 888 (s), 842 (m), 795 (m), 784 (m), 722 (s) cm^{-1}; elemental analysis calcd for $C_{52}H_{92}Mn_2N_8$(%): C 66.50, H 9.87, N 11.93; found C 66.15, H 9.98, N 11.22.

$[(CyNCHNCy)_2Mn(tmeda)]$ (**3**): A solution of *N*,*N*′-dicyclohexylformamidine (4.0 g, 19.4 mmol) in THF (150 mL) was stirred with excess KH. When the vigorous gas evolution had ceased, the suspension was boiled and stirred for 20 min. The solution was then filtered while still hot, cooled, and then transferred with a cannula to a suspension of [$MnCl_2$(tmeda)] [prepared from $[MnCl_2(thf)_2]$ (2.6 g, 9.7 mmol) and TMEDA (9.7 mmol) in THF (50 mL)]. The reaction mixture was boiled and filtered through celite and then concentrated to a small volume (30 mL). The mixture was kept at −30 °C for a few days to give colorless crystals of **3**. Yield: 1.7 g (3.0 mmol, 31 %); IR (Nujol mull, NaCl): $\tilde{\nu}$ = 1645 (s), 1582 (s), 1260 (s), 1235 (s), 1183 (m), 1150 (s), 1109 (s), 1069 (s), 1031 (m), 986 (s), 888 (s), 824 (s), 785 (s), 723 (m), 691 (m), 659 (m) cm^{-1}; elemental analysis calcd for $C_{32}H_{62}MnN_6$(%): C 65.65, H 10.67, N 14.35; found C 65.68, H 10.35, N 14.20; μ_{eff} = 5.61 μ_B.

$[\{Mn(CyNCHNCy)_2\}_2(\mu\text{-}O)]_2\cdot 2THF$ (**4**): A yellow solution of **2** (0.5 g , 0.5 mmol) in THF (30 mL) was treated with excess dry oxygen. The color of the reaction mixture changed to dark brown. The resulting solution was kept at room temperature for 4 days to give dark brown crystals of **4**. Yield 0.4 g (0.4 mmol, 77 %); IR (Nujol mull, NaCl): $\tilde{\nu}$ = 1658 (s), 1577 (s), 1548 (s), 1365 (s), 1342 (s), 1312 (s), 1299 (m), 1275 (m), 1259 (s), 1230 (s), 1189 (m), 1160 (s), 1149 (m), 1113 (s), 1097 (s), 1065 (s), 1028 (m), 1006 (m), 972 (w), 888 (s), 843 (w), 803 (s), 722 (s), 697 (m), 627 (s), 610 (s) cm^{-1}; elemental analysis calcd for $C_{60}H_{108}Mn_2N_8O_4$(%): C 64.61, H 9.76, N 10.05; found C 65.02, H 9.13, N 10.17.

Structural studies: Suitable crystals were mounted with a cooled viscous oil on thin glass fibers. Data were collected on a Bruker SMART 1k CCD diffractometer with 0.3° ω scans at 0.90 and 180° in ϕ. Cell constants were calculated from reflection data obtained from 60 data frames collected at different parts of the Ewald sphere. No absorption corrections were applied. The reflection data for **1** and **4** were uniquely consistent for the reported space group. No symmetry higher than triclinic was observed for **2.** The systematic absences in the reflection data for **3** were consistent for either *C*2*c* or *Cc* space groups. Solution in the centrosymmetric space group for **3** and in the centric option for **2** yielded chemically reasonable and computationally stable results of refinement. The structures were solved by direct methods, completed with subsequent Fourier synthesis, and refined with full-matrix least-squares procedures based on F^2.

The metal positions in **1** are located at the vertices of a tetrahedron with the oxygen atom O(100) located in the center. After initial location of the primary tetrahedron and ligand atoms, a secondary inverted tetrahedron became apparent from the remaining electron density peaks. Further inspection of the isotropic parameters of the $LiMn_3$ cluster suggested Li/Mn disorder. Refinement of the occupancies of the eight possible combinations yielded a final structure composed of six disordered contributions with a 68:13:10:4:3:2 distribution of the site occupancy. Similar disorder has been previously observed in a series of tetrahedral and tetranuclear oxo clusters that contain manganese.[20a] Two molecules of cocrystallized THF were located in the asymmetric unit, and were treated with noncrystallographic symmetry restraints. The compound molecule **3** was located on a twofold axis, while **4** was located on an inversion center. In the case of **4**, two molecules of cocrystallized THF are present in the asymmetric unit.

The solvent atoms of **1** were refined isotropically in order to conserve a reasonable data/parameter ratio. All other non-hydrogen atoms were refined with anisotropic displacement parameters. Hydrogen atoms were assigned with idealized geometry, and constrained with an isotropic, riding model. Crystallographic details are presented in Table 1. Selected bond lengths and angles are given in Table 2. All scattering factors are contained in the SHELXTL 5.03 program library (Sheldrick, **1997**, WI). Crystallographic data (excluding structure factors) for the structures reported in this paper have been deposited with the Cambridge Crystallographic Data Center as supplementary publication no. CCDC-101879 – 101882. Copies of the data can be obtained free of charge on application to CCDC, 12 Union Road, Cambridge CB2 1EZ, UK (fax: (+44) 1223-336-033; e-mail: deposit@ccdc.cam.ac.uk).

Table 1. Crystal data and results of the structure analysis.

	1	**2**	**3**	**4**
formula	$C_{86}H_{148}LiMn_3N_{12}O_4$	$C_{52}H_{92}Mn_2N_8$	$C_{32}H_{62}MnN_6$	$C_{60}H_{108}Mn_2N_8O_4$
formula weight	1582.02	938.21	585.82	1115.45
space group	$P2_1/c$	$P\bar{1}$	$C2/c$	$P2_1/n$
a [Å]	15.0061(8)	11.8399(6)	13.543(2)	10.6863(6)
b [Å]	19.531(1)	11.9788(6)	32.884(5)	14.2717(7)
c [Å]	31.116(2)	19.2152(9)	8.776(2)	20.7017(9)
α [°]		84.854(1)		
β [°]	94.468(1)	88.020(1)	120.059(9)	101.282(1)
γ [°]		82.783(1)		
V [Å^3]	9042.3(9)	2692.0(2)	3383(1)	3096.2(3)
Z	4	2	4	4
λ [K_α]	$Mo_{K\alpha}$	$Mo_{K\alpha}$	$Mo_K\alpha$	$Mo_{K\alpha}$
T [°C]	−125(2)	−75(2)	−73(2)	−75(2)
ρ_{calcd} [g cm^{-3}]	1.162	1.157	1.150	1.196
μ_{calcd} [cm^{-1}]	4.64	5.09	4.19	4.58
R,[a] wR_2,[b] GoF	0.0868, 0.2202, 1.020	0.0570, 0.1315, 1.96	0.0389, 0.1027,1.012	0.0763, 0.1935, 1.039

[a] $R = \Sigma ||F_o| - |F_c|| / \Sigma |F_o|$. [b] $R_w = [(\Sigma(|F_o| - |F_c|)^2 / \Sigma w F_o^2)]^{1/2}$

0947-6539/99/0502-0578 $ 17.50+.50/0 *Chem. Eur. J.* **1999**, *5*, No. 2

Table 2. Selected bond lengths [Å] and angles [°].

1		2		3		4	
Mn(11)–Mn(12)	3.1153(16)	Mn(1)–Mn(2)	3.172(2)	Mn–N(1)	2.177(2)	Mn–Mn(A)	2.5678(14)
Mn(11)–Mn(13)	3.1337(16)	Mn(1)–N(1)	2.155(2)	Mn–N(2)	2.348(2)	Mn–O(1)	1.804(3)
Mn(11)–Li(14)	3.296(5)	Mn(1)–N(2)	2.163(2)	Mn–N(3)	2.420(2)	Mn–N(1)	2.052(4)
Mn(12)–Li(14)	3.220(5)	Mn(1)–N(5)	2.104(2)	N(1)–C(13)	1.310(3)	Mn–N(2)	2.056(4)
Mn(13)–Li(14)	3.342(5)	Mn(1)–N(7)	2.134(2)	N(1)–C(6)	1.460(3)	Mn–N(3)	2.008(4)
Mn(11)–O(100)	2.012(4)	Mn(2)–N(3)	2.188(2)	N(1)-Mn-N(2)	60.23(8)	N(1)–C(13)	1.303(6)
Mn(12)–O(100)	1.987(4)	Mn(2)–N(4)	2.159(2)	N(1)-Mn-N(3)	154.27(9)	N(2)–C(13)	1.309(6)
Mn(13)–O(100)	1.992(4)	Mn(2)–N(6)	2.164(2)	N(1)-Mn-N(1a)	108.85(12)	N(3)–C(26)	1.319(6)
Li(14)–O(100)	1.962(6)	Mn(2)–N(8)	2.193(2)	N(1)-Mn-N(2a)	60.23(8)	N(4)–C(26)	1.325(6)
Mn(11)–N(11)	2.122(8)	N(1)–C(13)	1.324(3)	N(1)-Mn-N(3a)	91.27(9)	O(1A)-Mn-O(1)	89.18(14)
Mn(11)–N(4)	2.132(7)	N(2)–C(13)	1.313(4)	N(2)-Mn-N(2a)	164.27(11)	N(1)-Mn-N(2)	64.3(2)
Mn(11)–N(8)	2.151(6)	N(3)–C(26)	1.308(4)	N(3)-Mn-N(3a)	75.01(12)	N(4A)-Mn-N(1)	92.5(2)
Mn(12)–N(9)	2.075(6)	N(4)–C(26)	1.321(4)			O(1A)-Mn-N(4A)	88.1(2)
Mn(12)–N(7)	2.095(5)	N(5)–C(39)	1.320(3)			O(1)-Mn-N(3)	87.9(2)
Mn(12)–N(2)	2.271(6)	N(6)–C(39)	1.305(4)			N(3)-Mn-N(2)	92.3(2)
Mn(13)–N(3)	2.084(5)	N(7)–C(52)	1.328(4)			N(1)-C(13)-N(2)	113.6(5)
Mn(13)–N(1)	2.143(5)	N(8)–C(52)	1.300(4)			N(3)-C(26)-N(4)	127.3(5)
Mn(13)–N(5)	2.195(6)	N(1)-Mn(1)-N(2)	63.08(9)			C(26)-N(3)-C(19)	115.5(4)
Li(14)–N(12)	2.169(8)	N(7)-Mn(1)-N(2)	110.64(9)			C(26)-N(3)-Mn	119.4(3)
Li(14)–N(6)	2.201(7)	N(5)-Mn(1)-N(7)	117.29(9)			C(19)-N(3)-Mn	125.1(3)
Li(14)–N(10)	2.543(8)	N(5)-Mn(1)-N(1)	114.53(10)			C(13)-N(1)-C(6)	125.2(5)
N(1)–C(13)	1.333(8)	N(4)-Mn(2)-N(3)	62.60(9)			C(13)-N(1)-Mn	91.2(3)
N(2)–C(13)	1.319(8)	N(6)-Mn(2)-N(3)	104.33(9)			C(6)-N(1)-Mn	143.3(4)
O(100)-Mn(11)-N(11)	103.6(2)	N(4)-Mn(2)-N(8)	103.22(9)				
N(11)-Mn(11)-N(4)	112.6(3)	N(6)-Mn(2)-N(8)	132.87(9)				
N(11)-Mn(11)-N(8)	111.6(2)	N(2)-C(13)-N(1)	117.9(3)				
O(100)-Mn(11)-N(8)	107.47(18)	N(3)-C(26)-N(4)	118.4(3)				
N(2)-C(13)-N(1)	125.1(6)	N(6)-C(39)-N(5)	120.7(3)				
N(4)-C(26)-N(3)	125.9(6)	N(8)-C(52)-N(7)	120.6(3)				
N(6)-C(39)-N(5)	124.3(6)	C(13)-N(1)-C(6)	118.0(2)				
N(8)-C(52)-N(7)	126.4(6)	C(13)-N(1)-Mn(1)	89.5(2)				
N(9)-C(65)-N(10)	125.8(6)	C(6)-N(1)-Mn(1)	150.9(2)				
N(12)-C(78)-N(11)	125.7(7)	C(39)-N(5)-C(32)	116.7(2)				
		C(39)-N(5)-Mn(1)	110.7(2)				
		C(32)-N(5)-Mn(1)	129.3(2)				

Molecular orbital calculations: Semiempirical PM3 MO calculations were carried out with the geometrical parameters obtained from the crystal structures of **2** and **4** using a Silicon Graphics workstation and the Spartan 4.0 software package.[21] The program's default parameters were used for both calculations. The fractional atomic coordinates of the crystal structures were converted to the corresponding Cartesian coordinates with the XP program of the SHELXTL program library.

Results

As described in Scheme 1, the reaction of $[MnCl_2(thf)_2]$ with two equivalents of the *N*,*N*′-dicyclohexylformamidinate anion took two completely different pathways depending on the formamidinate alkali metal countercation employed (Li or K). The reaction with the lithium derivative proceeded rapidly at room temperature in THF to form good yields of a poorly soluble yellow compound which, upon boiling, redissolved in THF to afford pale orange, extremely air-sensitive crystals of a mixed-valence Mn^{II}/Mn^{III} oxo cluster $[Mn_3Li(CyNCHNCy)_6(\mu,\eta^3\text{-}O)]\cdot 2THF$ (**1**). The presence of lithium was clearly indicated by qualitative chemical analysis. The data from combustion analysis was in good agreement with the proposed formula. The IR spectrum did not show any particular features other than the presence of the characteristic bands of the *N*,*N*′-dicyclohexylformamidine ligand and

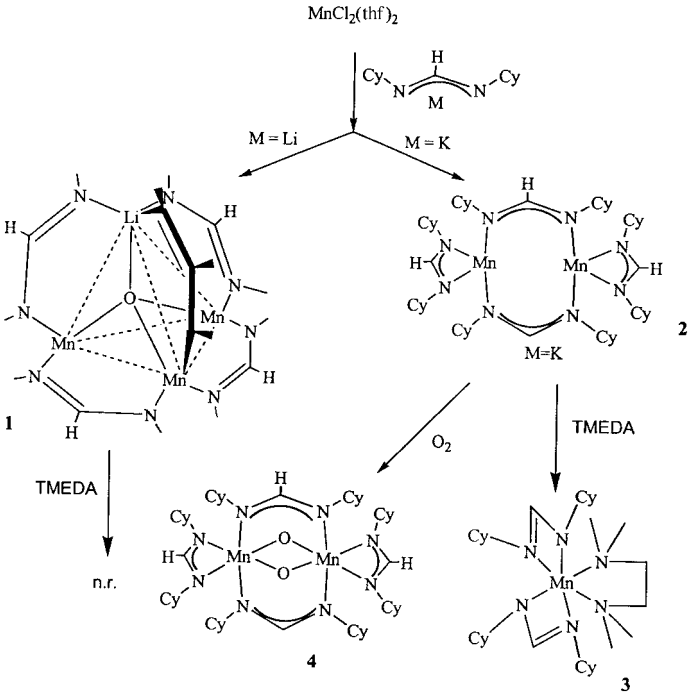

Scheme 1. The synthesis of complexes **1** and **2** from $[MnCl_2(thf)_2]$ and the lithium or potassium salts of *N*,*N*′-dicyclohexylformamidinate, respectively, and their subsequent reactions with TMEDA or O_2.

interstitial THF. The complex is paramagnetic with a magnetic moment significantly lower than that expected for the d^4 electronic configuration of Mn^{III}.

In contrast, the same reaction carried out under very similar conditions but with the potassium salt of the amidinate anion, gave a dinuclear Mn^{II} compound. The reaction, also carried out in THF, yielded pale yellow crystals of the dinuclear $[\{(CyNCHNCy)Mn\}_2(\mu\text{-}CyNCHNCy)_2]$ (**2**) after a short reflux and work up. The dimeric nature and the connectivity was elucidated by an X-ray crystal structure analysis. The data from combustion analysis was in good agreement with the proposed formula. The complex is paramagnetic with a room temperature magnetic moment slightly lower than that expected for a d^5 high-spin electronic configuration of Mn^{II}; this indicates that there is probably some magnetic coupling between the two metal centers. The behavior of the inverse of the magnetic susceptibility as a function of the temperature showed the characteristic behavior of an antiferromagnetically coupled complex (Figure 1) with a Neel temperature of

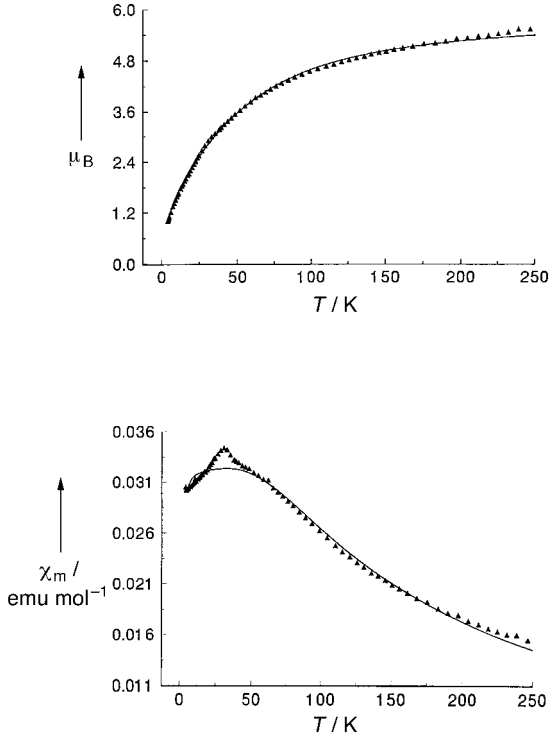

Figure 1. Plots of the magnetic susceptibility and of the magnetic moment against the temperature for complex **2** (continuous line shows the calculated trend).

30 K and an exchange coupling constant of $J = -5.18\ cm^{-1}$. In the region 60–273 K, the compound behaves as a regular paramagnet and follows the Curie Law with a nearly zero intercept [$\theta = -1$ K]. A reasonable fit of the experimental data (Figure 1) was obtained with an isotropic exchange equation derived from the van Vleck equation for a pair of $S = 5/2$ centers ($H = 2J\boldsymbol{S}_1\boldsymbol{S}_2$) and assuming the following parameters: g = 2.003, $J = -5.18\ cm^{-1}$, ferromagnetic, paramagnetic impurity = 0.022, $\theta = -1$ K, $R = 0.0168$, TIP = 0 [$R = \{\Sigma(\chi_{obs} - \chi_{calc})^2/\Sigma(\chi_{obs})^2\}^{1/2}$, θ = Weiss-like correction].

Treatment of **2** with TMEDA cleaved the dinuclear structure and produced a monomeric and octahedral compound $[(CyNCHNCy)_2Mn(tmeda)]$ (**3**). Conversely, the polynuclear structure of **1** was insensitive to TMEDA. Even reactions carried out with either Li or K, *N*,*N*′-dicyclohexylformamidinate, and $[MnCl_2(thf)_2]$ in the presence of TMEDA led to the formation of **1** or **3**, respectively, as the sole products. The same results were obtained by with $[MnCl_2(tmeda)]$. Complex **3** possesses a magnetic moment at room temperature which is slightly lower than that expected for the high spin d^5 electronic configuration of Mn^{II}.

Compounds **1** and **2** are both extremely sensitive to oxygen. Upon exposure to even traces of oxygen, an intensely dark reddish-brown color developed. Dark red crystals of a new compound, **4**, separated from the THF solution of **2** upon concentration and standing at room temperature. Attempts to identify the product of the reaction of **1** with O_2 led only to intractable materials. Analytical data were in agreement with the formulation $[(CyNCHNCy)Mn]_2(\mu\text{-}CyNCHNCy)_2(\mu\text{-}O)]_2$ (**4**), as elucidated by the X-ray crystal structure. The IR spectrum did not show any unusual features and was very similar to that of complex **2**, thus indicating that a relatively minor molecular reorganization had occurred during the reaction with O_2. The absence of absorptions in the region $\nu = 4500-2900\ cm^{-1}$ ruled out the possibility that **4** might be a hydroxo-bridged Mn^{III} compound.[19] The behavior of the magnetic susceptibility as a function of temperature (Figure 2) was considerably different from that of the antiferro-

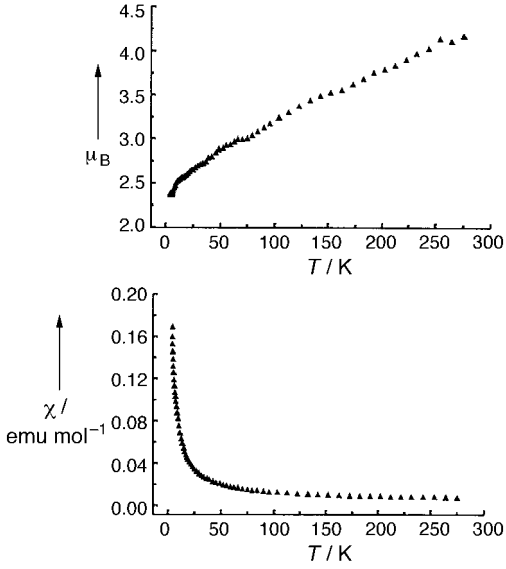

Figure 2. Plots of the magnetic susceptibility and of the magnetic moment against the temperature for complex **4**.

magnetically coupled **2**. The plot of $1/\chi$ against the temperature deviates significantly from the Curie–Weiss law and is curved in the range $T = 5-255$ K. The magnetic moment drops from 4.1 μ_B at 273 K to 2.3 μ_B at 5 K in an almost linear manner. While this is not indicative of ferromagnetism, antiferromagnetic coupling cannot be ruled out. The magnetic moment at room temperature is only slightly higher than that expected for a hexacoordinate high-spin d^3 system. At present we do not understand this unusual magnetic behavior and further studies on this system are underway.

0947-6539/99/0502-0580 $ 17.50+.50/0 *Chem. Eur. J.* **1999**, *5*, No. 2

Structural studies

Complex 1: One lithium and three manganese atoms form the core of the structure of **1** (Figure 3). The four metal atoms define a rather symmetric tetrahedron [Mn(11)-Mn(12)-Mn(13) 64.48(4), Mn(11)-Mn(12)-Li(14) 62.68(10), Mn(11)-Mn(13)-Li(14) 61.9(9), Mn(12)-Mn(13)-Li(14) 57.7(9)°] with significantly short nonbonding intermetallic contacts

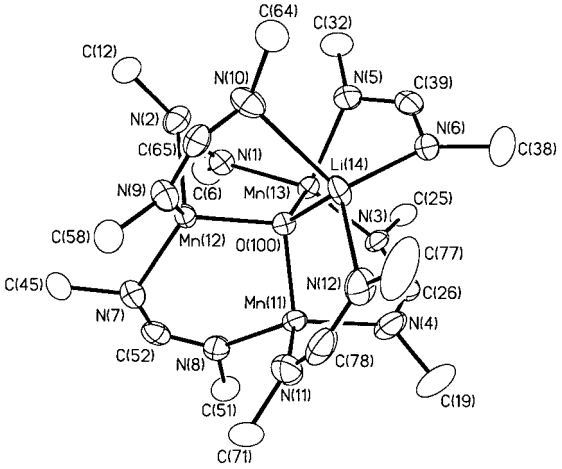

Figure 3. Structure of **1**. Thermal ellipsoids are drawn at the 30% probability level.

[Mn(11)···Mn(12) 3.115(2), Mn(11)···Mn(13) 3.134(2), Mn(12)···Mn(13) 3.334(2), Mn(11)···Li(1)4 3.296(5), Mn(12)–Li(14) 3.220(5), Mn(13)···Li(14) 3.342(5) Å]. Evidently, as a result of the disordered occupancy of the lithium atoms, all the core bond lengths and angles are averaged. The structure is completed by one oxygen atom placed in the center of the coordination tetrahedron [Mn(11)-O(100)-Mn(12) 102.3(3), Mn(12)-O(100)-Mn(13) 113.8(3), Mn(13)-O(100)-Li(14) 115.4(6), Li(14)-O(100)-Mn(11) 112.1(6)°] and six *N*,*N*′-dicyclohexylformamidinate groups. Each of the six formamidinate anions bridges two metals and adopts the characteristic three-center chelating geometry usually observed in lantern-type systems or in metal–metal-bonded structures of this type of ligand. One ligand is situated along each edge of the tetrahedral core [Mn(11)–N(11) 2.122(8), Mn(11)–N(4) 2.132(7), Mn(11)–N(8) 2.151(6), Mn(12)–N(9) 2.075(6), Mn(12)–N(7) 2.095(5), Mn(12)–N(2) 2.271(6), Mn(13)–N(3) 2.084(5), Mn(13)–N(1) 2.143(5), Mn(13)–N(5) 2.195(6), Li(14)–N(12) 2.169(8), Li(14)–N(6) 2.201(7), Li(14)–N(10) 2.543(8) Å]. However, in contrast to the multiply bonded systems of V[2b] and Cr[3c] of the same ligand, the formamidinate N-C-N array is *not* coplanar with the two bridged metals but it is skewed in order to accommodate the long intermetallic distance. As a result, some of the nitrogen atoms are no longer trigonal planar but assume a slightly pyramidal geometry. The two cyclohexyl rings of each *N*,*N*′-dicyclohexylformamidine have two opposite orientations with respect to the formamidinic hydrogen atom in order to minimize the H···H repulsions. The distances between the oxygen located in the center of the tetrametallic core and the three manganese atoms [Mn(11)–O(100) 2.012(4), Mn(12)–O(100) 1.987(4), Mn(13)–O(100) 1.992(4) Å] and the lithium atom [Li(14)–O(100) 1.962(6) Å] are averaged as a result of the disorder of the Mn_3Li core. Two molecules of interstitial THF complete the crystal structure.

Complex 2: The dinuclear frame of **2** is formed by two distorted tetrahedral manganese atoms [N(1)-Mn(1)-N(2) 63.08(9), N(2)-Mn(1)-N(7) 110.64(9), N(7)-Mn(1)-N(5) 117.29(9), N(5)-Mn(1)-N(1) 114.53(10)°] (Figure 4) connected

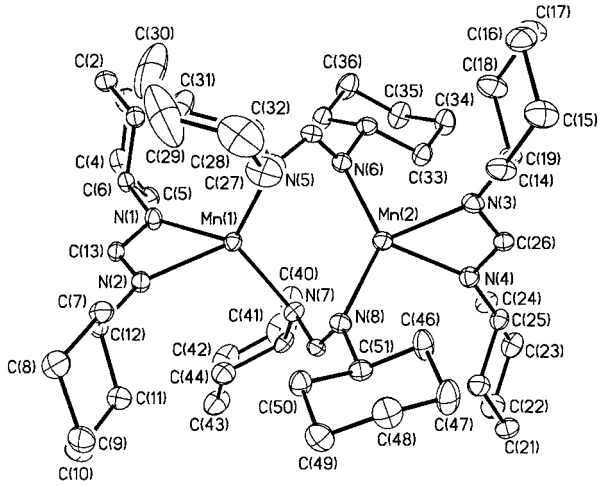

Figure 4. Structure of **2**. Thermal ellipsoids are drawn at the 30% probability level.

together by two bridging formamidinate ligands [Mn(1)–N(5) 2.104(2), Mn(1)–N(7) 2.134(2), Mn(2)–N(6) 2.164(2), Mn(2)–N(8) 2.193(2) Å].[20b] Two other formamidinate anions, which adopt a regular chelating geometry [Mn(1)–N(1) 2.155(2), Mn(1)–N(2) 2.163(2), Mn(2)–N(3) 2.188(2), Mn(2)–N(4) 2.159(2) Å], are bonded to the two metals and define the tetrahedral coordination geometry around each manganese atom. The two bridging *N*,*N*′-dicyclohexylformamidinates adopt the usual three-center chelating bonding mode. However, similar to the case of complex **1**, the amidinate N-C-N backbone is not coplanar with the two metal centers; it is severely skewed to allow the distortion necessary to accommodate the long intermetallic distance [Mn(1)-N(5)-C(39)-N(6) 34.0, Mn(1)-N(7)-C(52)-N(8) 47.0, Mn(2)-N(6)-C(39)-N(5) 45.4, Mn(2)-N(8)-C(52)-N(7) 36.4°]. To accommodate the sp^2 hybridization of the formamidine C atom [N(5)-C(39)-N(6) 120.7(3), N(7)-C(52)-N(8) 120.6(3)°], the *ipso* hydrogen atoms of the two cyclohexyl rings point towards the inside and the outside of the molecular center, respectively. The hydrogen atom pointing to the exterior of the molecules forms a short H···H nonbonding contact [H···H 2.13 Å] with the formamidinic hydrogen atom. As a result, the nitrogen donor atoms are no longer trigonal planar but slightly pyramidal [C(32)-N(5)-C(39) 116.7(2), C(39)-N(5)-Mn(1) 110.7(2), Mn(1)-N(5)-C(32) 129.3(2), C(39)-N(6)-C(38) 117.2(2), C(39)-N(6)-Mn(2) 102.3(2), C(38)-N(6)-Mn(2) 129.7(2); Mn(1)-N(7)-C(52) 110.7(2), C(52)-N(7)-C(45) 115.7(2), C(45)-N(7)-Mn(1) 123.2(2); C(52)-N(8)-C(51) 116.6(2), C(51)-N(8)-Mn(2) 137.0(2), Mn(2)-N(8)-

C(52) 95.3(2)°]. The Mn–Mn distance [Mn(1)···Mn(2) 3.1701(6) Å] is rather long and outside the bonding range.

Complex 3: The structure consists of a slightly distorted octahedral manganese atom [N(1)-Mn-N(2) 60.23(8), N(1)-Mn-N(3) 154.27(9), N(2)-Mn-N(3) 98.47(8)°] surrounded by two amidinate anions [Mn–N(1) 2.177(2), Mn–N(2) 2.348(2) Å] and one TMEDA molecule (Figure 5). Both

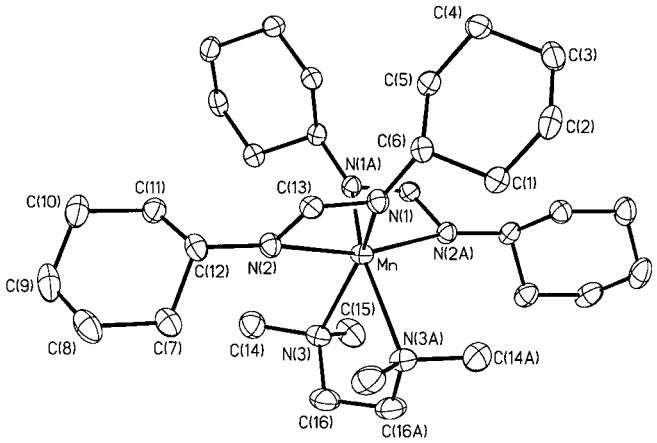

Figure 5. Structure of **3**. Thermal ellipsoids are drawn at the 30% probability level.

ligands adopt a regular chelating bonding mode [N(1)-C(13)-N(2) 120.7(3)°] to produce planar four-membered metallacycles [torsion angle Mn-N(1)-C(13)-N(2) 7.6°]. The two nitrogen atoms of one chelating TMEDA complete the structure [Mn–N(3) 2.420(2), N(3)-Mn-N(3a) 75.01(12)°]. The three metallacycles formed by the two amidinates and the TMEDA molecule with the metal center adopt an overall propellerlike conformation in order to minimize the steric repulsions. Also the *ipso* hydrogen atoms of the cyclohexyl rings are coplanar with the formamidine hydrogen atom and have rather short H···H contacts [H(13a)···H(6a) 2.2, H(13a)···H(12a) 2.1 Å].

Complex 4: The dinuclear frame is composed of two manganese atoms with a distorted octahedral coordination [O(1)-Mn-O(1A) 89.18(14), O(1A)-Mn-N(4A) 88.1(2), N(4A)-Mn-N(1) 92.5(2), N(1)-Mn-N(2) 64.3(2), N(2)-Mn-N(3) 92.3(2), N(3)-Mn-O(1) 87.9(2)°] linked together by two bridging oxygen atoms [Mn–O(1) 1.804(3) Å] and two bridging *N,N′*-dicyclohexylformamidinate anions [Mn–N(3) 2.008(4), Mn–N(4A) 2.013(4) Å] in an overall edge-sharing bioctahedral structure (Figure 6). Two other formamidinate anions, which adopt a normal chelating geometry [Mn–N(1) 2.052(4), Mn–N(2) 2.056(4) Å], complete the octahedral coordination sphere around each manganese atom. Therefore, the coordination geometry of each manganese atom is defined as follows. Two bridging oxygen and two nitrogen atoms of one chelating *N,N′*-dicyclohexylformamidinate [N(1)-Mn-O(1A) 102.7(2), O(1A)-Mn-O(1) 89.18(14), O(1)-Mn-N(2) 103.8(2), N(2)-Mn-N(1) 64.3(2)°] define the equatorial plane. Two nitrogen atoms of the two bridging formamidinate anions occupy the two axial positions [N(3)-

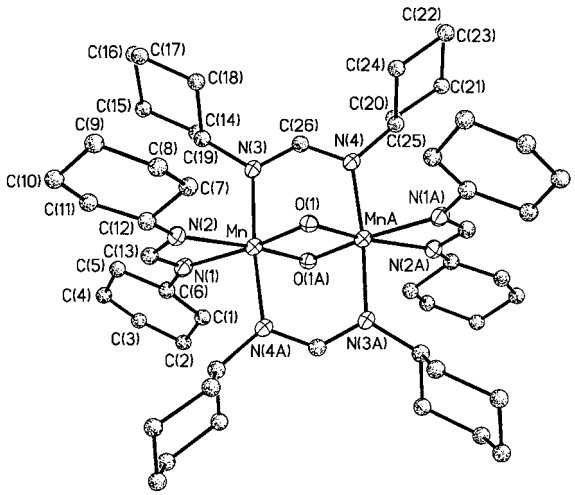

Figure 6. Structure of **4**. Thermal ellipsoids are drawn at the 30% probability level.

Mn-N(4A) 174.3(2)°]. The bridging amidinates adopt the normal three-center chelating geometry in which the N-C-N array is almost coplanar with the Mn–Mn vector [Mn-N(3)-C(26)-N(4) −1.8 and Mn(A)-N(4)-C(26)-N(3) 1.5°]. The nitrogen donor atoms have distorted trigonal planar coordination [C(1)9-N(3)-C(26) 115.5(4), C(26)-N(3)-Mn 119.4(3), Mn-N(3)-C(19) 125.1(3); C(26)-N(4)-C(25) 114.6(4), C(25)-N(4)-Mn(A) 126.4(3), Mn(A)-N(4)-C(26) 119.0(3)]. The central Mn_2O_2 core is planar [Mn-O(1)-Mn(A)-O1(A) 0.0] and coplanar with the four nitrogen atoms of the terminal chelating formamidinate ligands [N(2)-Mn-O(1)-Mn(A) 0.0, N(1)-Mn-O(1)-Mn(A) 0.0°].

Molecular orbital calculations

Complex 2: Given that the magnetic moment was slightly lower than that expected for the d^5 electronic configuration of high-spin tetrahedral manganese atoms, a multiplicity of nine was considered to be the most appropriate for the calculation. The geometrical distortion of the bridging formamidinate ligands and consequent lack of symmetry is reflected in the divergent participation of the atomic orbitals of the two manganese atoms in the formation of the MOs. The calculation yielded a considerable HOMO–LUMO gap (5.8 eV) and four nearly degenerate frontier orbitals (HOMO, HOMO-1, HOMO-2, and HOMO-3). These four orbitals largely account for the bonding with the chelating formamidine and are mainly nonbonding or antibonding with respect to the Mn–Mn interaction. Among the large number of molecular orbitals present, a few are worth particular attention (Figure 7): two almost degenerate molecular orbitals, HOMO-23 and HOMO-25, located at −13.8 and −13.9 eV, respectively, have the shape of two Mn–Mn σ bonds. These two orbitals are chiefly formed by two d-centered hybrid combinations. However, in spite of the fact that the lobes lying on the intermetallic vector in both MOs possess the appropriate phase and orientation for the formation of a σ bond, the overlap is negligible. Conversely, the amidinate nitrogen p orbitals participate significantly in the formation of the MOs. A direct Mn–Mn interaction is also observed in HOMO-56,

0947-6539/99/0502-0582 $ 17.50+.50/0 *Chem. Eur. J.* **1999**, *5*, No. 2

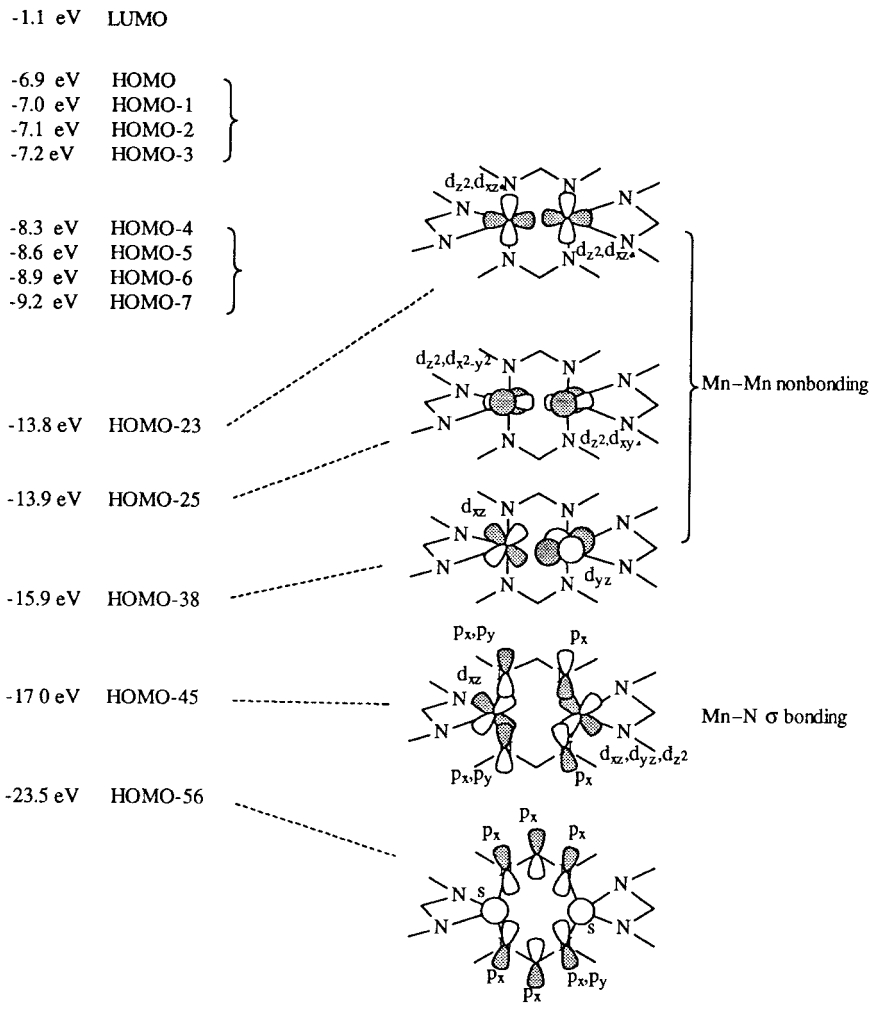

Figure 7. Semiempirical molecular orbitals in complex **2**.

located at −23.5 eV, which may be regarded as a sort of ligand-supported M–M bond. The orbital originates from the overlap of the manganese s orbitals with the p_x/p_y hybrid combination of the bridging formamidinate nitrogen and carbon orbitals and is a largely delocalized lobe situated in the center of the molecular core. However, the three Mn–Mn interactions do not produce any significant formal Mn–Mn bond order (0.06). The bonding of the Mn atoms with the bridging formamidinate Mn–N σ-bonding is mainly realized with HOMO-45 (−17.0 eV).

Complex 4: A multiplicity of seven was used in the calculation to account for the d^5 electronic configuration of the two metal centers. The Mn–Mn vector was imposed as a *z* axis for the calculation. In a similar manner to complex **2**, the HOMO–LUMO gap was significantly large (7.6 eV). The first five frontier orbitals (HOMO to HOMO-4) are uniformly spread between −7.2 and −7.8 eV, and, with the exception of HOMO-2, are nonbonding MOs or mainly ligand orbitals. The near D_{2h} symmetry of the complex is responsible for the presence of the large number of symmetric molecular orbitals which neatly accounts for the Mn–Mn, Mn-O-Mn and Mn-amidine-Mn interactions. The direct Mn–Mn interactions are provided by three MOs (Figure 8); these, however, always require the substantial participation of the bridging ligands and do not produce any chemically significant Mn–Mn bond (calculated Mn–Mn bond order = 0.022). Therefore, given the negligible direct overlap between the Mn atomic orbitals, these MOs may be perhaps better regarded as Mn–Mn nonbonding orbitals. The first, HOMO-9 (−10.2 eV) arises from the overlap of the two d_{xz} atomic orbitals oriented to form a Mn–Mn π bond. However, instead of giving direct overlap, these two atomic orbitals mix with the bridging *N*,*N*′-dicyclohexylformamidine p_x nitrogen orbitals to form Mn–N bonds. A similar scenario can be observed with HOMO-39 (−15.7 eV) which is formally a Mn–Mn σ-bond interaction. The MO is formed by the overlap of the d_{z^2} orbitals of the two Mn atoms. The Mn–Mn interaction is realized exclusively with the bridging oxygen p_y orbitals which, by the orientation of the lobe towards the center of the molecular core, gives rise to a largely delocalized circular lobe in the center of the molecule. The very next orbital (HOMO-40, −17.8 eV) is formed by the overlap of the lobes of the two d_{xz} orbitals above and below the plane of the Mn_2O_2 core and which form, with the participation of the oxygen p_x orbitals, two rings on the two sides of the Mn_2O_2 nodal plane. Five MOs are purely Mn-O-Mn bonds. The first (HOMO-2 −7.6 eV) is a Mn-O-Mn σ bond and originates from the overlap of the hybrid combination p_z, d_{z^2}, and $d_{x^2-y^2}$ of the two Mn atoms, with the p_z orbitals of the bridging oxygens. The next orbital (HOMO-20, −13.1 eV) arises from the side-on overlap of the lobes of $d_{x^2-y^2}$,d_{z^2} hybrid combinations located perpendicularly to the Mn–Mn axis and lying on the Mn_2O_2 core with the bridging oxygen p_y orbitals. The other two orbitals (HOMO-36 and HOMO-38 located at −14.8 and −15.2, respectively) are very similar and arise from the overlap of the Mn d_{yz} orbitals with either the p_y or p_z orbitals of oxygen. The last orbital is located at a very low energy (HOMO-68, −33.3 eV) and arises from the overlap of the d_{yz} orbitals with the bridging oxygen s orbitals to form two large lobes along the two Mn-O-Mn arrays. The Mn-amidine-Mn interactions deserve special attention: there are many molecular orbitals that account for these bonding interactions; however, four show a particularly extended delocalization along the Mn-N-C-N-Mn frameworks. These orbitals display a marked δ, π, and σ character. The first orbital (HOMO-48, −17.8 eV) is a large δ-orbital and is realized by the overlap of the Mn d_{xy} orbitals

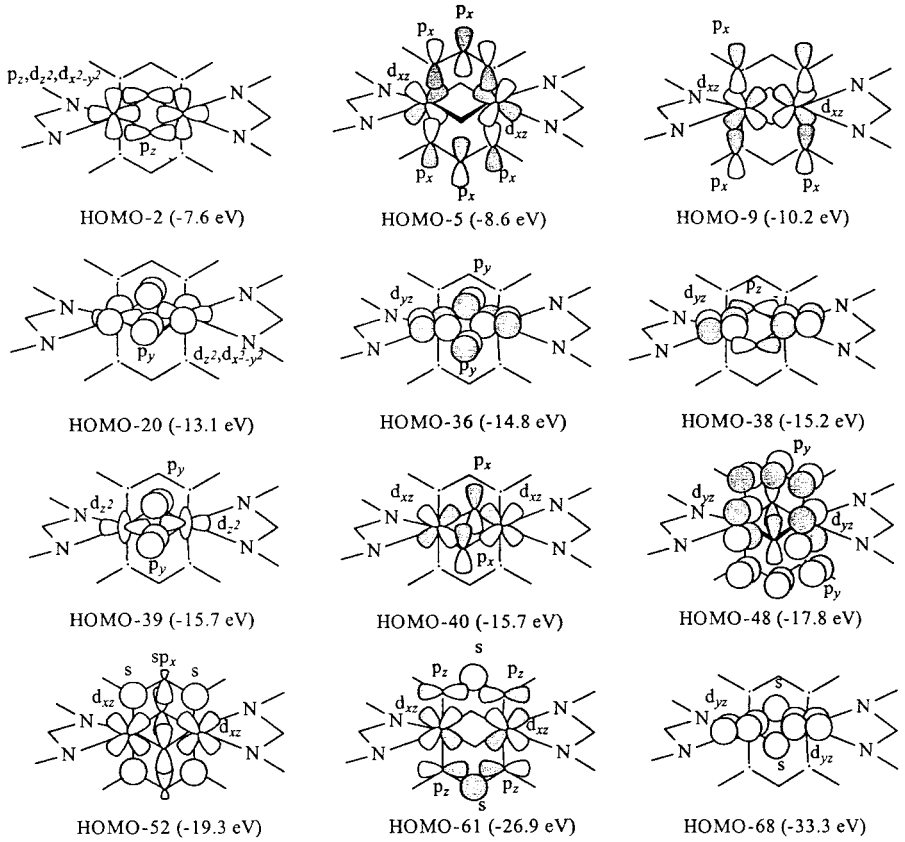

Figure 8. Semiempirical molecular orbitals in complex **4**.

with the π system of the two bridging formamidine ligands, thus forming four delocalized lobes placed symmetrically in the four regions defined by the Mn_2O_2 and Mn_2N_4 nodal planes. The orbital is formed by the mixing of the p_y orbitals of the formamidine N and C atoms with the d_{xy} orbtals of the two Mn atoms. The next orbital (HOMO-52 −19.3 eV) has, in contrast, a strong π character and is formed by the Mn d_{xz} atomic orbitals with nitrogen s orbitals. The formamidine carbon atoms contribute to the MO by means of sp_x hybrid combinations. In addition, the bridging oxygen atoms significantly participate in the molecular orbital with the p_x orbitals, thus contributing to the overall formation of two largely delocalized lobes on the two sides of the Mn_2O_2 nodal plane. The third orbital is also a π orbital [HOMO-61, −26.8 eV] and is formed by the overlap of the Mn d_{yz} orbitals with the bridging formamidine p_z orbitals of the nitrogen atoms and the s orbitals of the amidinate carbon atoms to produce two lobes which cover the two Mn-N-C-N-Mn arrays on the two sides of the Mn_2O_2 nodal plane. The last orbital is a Mn–amidinate σ orbital [HOMO-73, −42.3 eV], which arises from the simultaneous overlap of all the s orbitals of all the atoms participating in the formation of the core, to produce one unique lobe delocalized over the entire molecule.

Discussion

Deoxygenation of THF is likely to be at the origin of the formation of the oxo center in complex **1**. This idea is supported by the fact that substantial amounts of *n*-butane were consistently detected in the reaction mixtures of reproducible reactions. It should be also mentioned that the *N*,*N*′-dicyclohexylformamidinate lithium salt used in this work was repeatedly prepared following the procedure normally used for the preparation of Ti,[22] V,[2b] and Cr[3c] derivatives of the same ligand.

There are several precedents in the literature that describe reactions involving transition metals which lead to the fragmentation of THF.[23] A combination of high oxophilicity and a strongly reducing transition metal is typically observed when this phenomenon occurs. A transition metal system capable of donating two electrons to the THF molecule leads to oxygen abstraction with formation of metal–oxo derivatives and ethylene (not observed even in traces during the formation of **1**). Conversely, the donation of one electron by the transition metal usually fragments THF to afford the enolate anion and ethane, or a mixture of ethylene and hydrogen, or a combination of both possibilities. In only one case, the fragmentation to an ynolate anion and ethane was reported.[24] In this case, the ring-cleavage process was driven by a Lewis acid and did not require electrons to be added or removed from THF. A different pattern of fragmentation was observed in the case of an yttrium compound: it produced ethoxide and ethylene.[25] The two electrons required by this process were probably the result of an oxidation of the ligand. The formation of *n*-butane as the only volatile component in the mother liquor of **1** also requires two electrons and two hydrogen atoms. However, the formation of **1** (a mixed valence $Mn^{II}/Mn^{II}/Mn^{III}$ compound) provides only one electron, which indicates that the deoxygenation of THF is the result of a more complex reaction pathway. The possibility that oxidation of *N*,*N*′-dicyclohexylformamidinate may be the source of electrons was ruled out by the absence of *N*,*N*′-cyclohexylcarbodiimide in the reaction mixture.

It is rather surprising that the presence of a different countercation for the formamidinate anion (potassium instead of lithium) changes the reaction pathway so dramatically. On the other hand, lithium and potassium do indeed display very different Lewis acidities and polarizing abilities in an anhydrous environment. It is well known that the Lewis acidity of the metal plays a very fundamental role in the cleavage of THF and possibly in deoxygenation reactions. Furthermore, while the dinuclear frame of **2** is readily cleaved by treatment with TMEDA to afford the octahedral mononuclear complex **3**, the oxo derivative **1** did not react with

0947-6539/99/0502-0584 $ 17.50+.50/0 *Chem. Eur. J.* **1999**, *5*, No. 2

TMEDA. Treatment of the cluster **1** with TMEDA or even the reaction of preformed [$MnCl_2$(tmeda)] with the formamidinate lithium salt always led to **1**. This suggests that the incorporation of lithium in cluster **3** provides stability and is, perhaps, the thermodynamic driving force for the deoxygenation of THF.

Complex **2** displays a rather strong antiferromagnetic coupling between the two Mn centers. The magnetic moment at room temperature is consistent with the presence of about eight unpaired electrons per unit formula. The HOMO–LUMO separation (5.8 eV) is very large and is in good agreement with the fact that the magnetic moment shows a tendency to reach a plateau at higher temperatures. The high-lying orbitals (HOMO-1, HOMO-2, and HOMO-3) are nearly degenerate or are sufficiently close in energy to the HOMO, while the next MO (HOMO-4) is separated by a larger energy gap (1.1 eV). Perhaps this distribution of energy levels could explain the diamagnetism observed at temperatures below 30 K, in which all the electrons are coupled in the levels up to HOMO-4. At higher temperatures, the thermal depopulation promotes electron density in the next four orbitals and is thus responsible for the continuous variation of the magnetic moment up to the value found at room temperature (which indicates the presence of about eight unpaired electrons per formula unit).

The formation of complex **4** is the result of the addition of one molecule of oxygen to **2**. The four electrons necessary for the cleavage of O_2 are provided by the two-electron oxidation of the two Mn centers, probably through a one-step process. As indicated by the crystal structure, complex **2** has two small pockets on the two sides of the intermetallic vector which are ready to accommodate one molecule of dioxygen. The high-spin d^3 electronic configuration of the tetravalent manganese, which results from the two-electron oxidation of the two metal centers, strongly favors an octahedral geometry. Thus, the complex adopts the expected edge-sharing bioctahedral structure with two bridging oxo atoms and a fairly short Mn–Mn distance, which falls into the range found in other M_2O_2 cores.[26] The fairly short M–M distance allows the bridging *N*,*N*′-dicyclohexylformamidinate ligands to relax the distortion and to become coplanar with the M_2 vector. Only some minor distortions can still be observed in the bridging formamidinate ligands whose resting position typically requires much shorter M–M distances.

Acknowledgments

This work was supported by the Natural Science and Engineering Council of Canada (NSERC) and NATO (travel grant). Prof. Gilles Lamarche is gratefully acknowledged for his assistance with the magnetic measurements and for making available a low-field SQUID magnetometer.

[1] a) A. Littke, N. Sleiman, C. Bensimon, D. S. Richeson, *Organometallics* **1998**, *17*, 446; b) M. P. Coles, R. F. Jordan, *J. Am. Chem. Soc.* **1997**, *119*, 8125; c) J. C. Flores, J. C. W. Chien, M. D. Rausch, *Organometallics* **1995**, *14*, 1827; d) J. C. Flores, J. C. W. Chien, M. D. Rausch, *Organometallics* **1995**, *14*, 2106; e) D. Herskovicskorine, M. S. Eisen, *J. Organomet. Chem.* **1995**, *503*, 307; f) D. Walther, R. Fisher, H. Gorls, J. Koch, B. Scweder, *J. Organomet. Chem.* **1996**, *508*, 13.

[2] a) J. R. Hagadorn, J. Arnold, *J. Am. Chem. Soc.* **1996**, *118*, 893; b) S. Hao, P. Berno, R. K. Minhas, S. Gambarotta, *Inorg. Chim. Acta.* **1996**, *244*, 37; c) P. Berno, S. Hao, R. K. Minhas, S. Gambarotta, *J. Am. Chem. Soc.* **1994**, *116*, 7417; d) J. R. Hagadorn, J. Arnold, *Organometallics* **1998**, *17*, 1355.

[3] See, for example: a) F. A. Cotton, R. A. Walton, *Multiple Bonds Between Metal Atoms*, Oxford University Press, Oxford, UK, 2nd ed., **1992**; b) F. A. Cotton, L. M. Daniels, C. A. Murillo, *Angew. Chem.* **1992**, *104*, 795; *Angew. Chem. Int. Ed. Engl.* **1992**, *31*, 737; c) S. Hao, S. Gambarotta, C. Bensimon, J. J. H. Edema, *Inorg. Chim. Acta.* **1993**, *213*, 65.

[4] a) F. A. Cotton, X. Feng. C. A. Murillo, *Inorg. Chim. Acta* **1997**, *256*, 303; b) F. A. Cotton, L. M. Daniels, D. J. Maloney, J. H. Matonic, C. A. Murillo, *Inorg. Chim. Acta* **1997**, *256*, 283; c) E. Rotondo, G. Bruno, F. Nicolo, S. L. Schiavo, P. Piraino. *Inorg. Chem.* **1991**, *30*, 1195; d) D. Stalke, M. Wedler, F. T. Edelmann, *J. Organomet. Chem.* **1992**, *431*, C1.

[5] a) D. G. Dick, R. Duchateau, J. J. H. Edema, S. Gambarotta, *Inorg. Chem.* **1993**, *32*, 1959; b) J. R. Hagadorn, J. Arnold, *Inorg. Chem.* **1997**, *36*, 132; c) M. Westerhausen, W. Schwarz, *Z. Anorg. Allg. Chem.* **1993**, *619*, 1455;

[6] F. T. Edelmann, *Coord. Chem. Rev.* **1994**, *133*, 219.

[7] a) Y. Zhou, D. S. Richeson, *Inorg. Chem.* **1996**, *35*, 1423; b) Y. Zhou, D. S. Richeson, *Inorg. Chem.* **1996**, *35*, 2448; c) Y. Zhou, D. S. Richeson, *J. Am. Chem. Soc.* **1996**, *118*, 10850; d) Y. Zhou, D. S. Richeson, *Inorg. Chem.* **1997**, *36*, 501; e) S. R. Foley, C. Bensimon, D. S. Richeson, *J. Am. Chem. Soc.* **1997**, *119*, 10359.

[8] a) M. Wedler, M. Noltemeyer, U. Pieper, H.-G. Schmidt, D. Stalke, F. T. Edelmann, *Angew. Chem.* **1990**, *102*, 941; *Angew. Chem. Int. Ed. Engl.* **1990**, *29*, 894; b) R. Duchateau, C. T. Van Wee, A. Meetsma, J. H. Teuben, *J. Am. Chem. Soc.* **1993**, *115*, 4931.

[9] a) M. Wedler, H. W. Roesky, F. T. Edelmann, *J. Organomet. Chem.* **1988**, 345, C1; b) M. Wedler, M. Noltemeyer, F. T. Edelmann, *Angew. Chem.* **1992**, *104*, 64; *Angew. Chem. Int. Ed. Engl.* **1992**, *31*, 72; c) M. Wedler, F. Knosel, F. T. Edelmann, U. Behrens, *Chem. Ber.* **1992**, *125*, 1313.

[10] K. Köhler, H. W. Roesky, M. Noltmeyer, H. C. Schmidt, C. F. Erdbrüger, G. M. Sheldrick, *Chem. Ber.* **1993**, *126*, 921.

[11] For reviews and review articles see, for example: a) V. L. Pecoraro, *Photochem. Photobiol.* **1988**, *48*, 249; b) M. Mulay, S. Padhye, *Proc. Indian Natl. Sci. Acad.* **1987**, *B53*, 471; c) J. B. Vincent, G. Christou, *Adv. Inorg. Chem.* **1989**, *33*, 197; d) K. Wieghardt, *Angew. Chem.* **1989**, *101*, 1179; *Angew. Chem. Int. Ed. Engl.* **1989**, *28*, 1153; e) G. W. Brudvig, R. H. Crabtree, *Prog. Inorg. Chem.* **1989**, *37*, 99; f) M. Stebler, A.Ludi, H. B. Burgi, *Inorg. Chem.* **1986**, *25*, 4743; g) G. Christou, *Acc. Chem. Res.* **1989**, *22*, 328.

[12] a) S. Amesz, *J. Biochim. Biophys.* **1983**, *726*, 1; b) Y. Takohashi, S. Katoh, *Biochim. Biophys. Acta.* **1986**, *848*, 183; c) N. Tamura, M. Ikeuchi, Y. Inoue, *Biochim. Biophys. Acta.* **1989**, *973*, 281; d) R. D. Guiles, J. L. Zimmerman, A. E. McDermott, V. K. Yachandra, J. L. Cole, S. L. Dexheimer, R. D. Britt, K. Wieghardt, U. Bossek, K. Sauer, M. P. Klein, *Biochemistry* **1990**, *29*, 471; e) V. J. De Rose, V. K. Yachandra, A. E. McDermott, R. D. Britt, K. Sauer, M. D. Klein, *Biochemistry* **1991**, *30*, 1335.

[13] C. K. Vance, A. F. Miller, *J. Am. Chem. Soc.* **1998**, *120*, 461.

[14] See, for example: a) H. J. Eppley, S. M. J. Aubin, W. E. Streib, J. C. Bollinger, D. N. Hendrickson, G. Christou, *Inorg.Chem.* **1997**, 36, 109; b) V. A. Grillo, M. J. Knapp, J. C. Bollinger, D. N. Hendrickson, G. Christou, *Angew. Chem.* **1996**, *108*, 1962; *Angew. Chem. Int. Ed. Engl.* **1996**, *35*, 1818; c) S. Pal, M. M. Olmstead, W. H. Armstrong, *Inorg. Chem.* **1995**, *34*, 4708; d) K. R. Reddy, M. V. Rajasekharan, S. Padhye, F. Dahan, J. -P. Tuchagues, *Inorg.Chem.* **1994**, *33*, 428; e) L. Stelzig, A. Steiner, B. Chansou, J. P. Touchagues, *Chem. Commun.* **1998**, 771.

[15] a) S. Hao, P. Berno, R. Minhas, S. Gambarotta, *Inorg. Chim. Acta* **1996**, *244*, 37; b) A. H. Saeed, A. S. Sellman, *J. Spectrosc.* **1990**, *29*, 123.

[16] P. Boudjouk, J. So, *Inorg. Synth.* **1992**, *29*, 108.

[17] M. B. Mabbs, D. Machin, *Magnetism and Transition Metal Complexes*, Chapman and Hall, London, **1973**.

[18] G. Foese, C. J. Gorter, L. J. Smits, *Constantes Selectionnes, Diamagnetisme, Paramagnetisme Relaxation Paramagnetique*, Masson, Paris, **1957**.

[19] F. M. MacDonnell, N. L. Fackler, C. Stern, T. V. O'Halloran, *J. Am. Chem. Soc.* **1994**, *116*, 7431.
[20] a) F. A. Cotton, L. M. Daniels, L. R. Falvello, J. H. Matonic, C. A. Murillo, X. Wang, H. Zhou, *Inorg. Chim. Acta* **1997**, *266*, 91; b) similar distortion was recently observed in a Fe complex: F. A. Cotton, L. M. Daniels, J. H. Matonic, C. A. Murillo, *Inorg. Chim. Acta.* **1997**, *256*, 277.
[21] All the calculations were performed with the software package *SPARTAN4.0,* Wavefunction, Inc.; 18401 Von Karman Ave., 370, Irvine, CA 92715 (USA), **1995**.
[22] S. Hao, K. Feghali, S. Gambarotta, *Inorg. Chem.* **1997**, *36*, 1745.
[23] See, for example: a) J. Jubb, S. Gambarotta, *Inorg. Chem*. **1994**, *33*, 2503; b) H. C. Aspinall, M. R. Tillotson, *Inorg. Chem.* **1996**, *35*, 2163; c) W. J. Evans, R. Dominguez, T. P. Hanusa, *Organometallics* **1986**, *5*, 12912.
[24] J. Jubb, S. Gambarotta, *J. Am. Chem. Soc*. **1993**, *115*, 10410.
[25] J. Jubb, S. Gambarotta, R. Duchateau, J. Teuben, *J. Chem. Soc. Chem. Commun.* **1994**, 2641.
[26] a) Z. Duan, M. Schmidt, V. G. Young, X. Xie, R. E. McCarley, J. G. Verkade, *J. Am. Chem. Soc*. **1996**, *118*, 5302; b) K. B. P. Ruppa, K. Feghali, I. Kovacs, K. Aparna, S. Gambarotta, G. P. A. Yap, C. Bensimon, *J. Chem. Soc. Dalton Trans.* in press.

Received: June 12, 1998 [F 1202]

0947-6539/99/0502-0586 $ 17.50+.50/0 *Chem. Eur. J.* **1999**, *5*, No. 2